JOURNAL OF SYNCHROTRON RADIATION

ISSN 1600-5775

Third-order nonlinear and linear time-dependent dynamical diffraction of X-rays in crystals

Minas K. Balyan*

Faculty of Physics, Department of Solid State Physics, Yerevan State University, Alex Manoogian 1, Yerevan 0025, Armenia. *Correspondence e-mail: mbalyan@ysu.am

Received 2 November 2015
Accepted 30 May 2016

Edited by A. Momose, Tohoku University, Japan

Keywords: third-order nonlinearity; time-dependent propagation equations; dynamical diffraction; X-ray pulse.

For the first time the third-order nonlinear time-dependent Takagi's equations of X-rays in crystals are obtained and investigated. The third-order nonlinear and linear time-dependent dynamical diffraction of X-rays spatially restricted in the diffraction plane pulses in crystals is investigated theoretically. A method of solving the linear and the third-order nonlinear time-dependent Takagi's equations is proposed. Based on this method, results of analytical and numerical calculations for both linear and nonlinear diffraction cases are presented and compared.

1. Introduction

For high-intensity radiation, theoretical and experimental investigations of nonlinear diffraction and other nonlinear effects of monochromatic waves are provided for X-ray synchrotron sources and X-ray free-electron lasers (XFELs). For these sources it is necessary to consider not only the diffraction of monochromatic waves: investigation of the time-dependent diffraction of X-ray pulses becomes essential. X-ray linear dynamical diffraction of monochromatic waves is described by Takagi's equations (Takagi, 1969). Linear time-dependent dynamical diffraction of X-rays in crystals is described by the time-dependent Takagi's equations. These equations for perfect and deformed crystals were first obtained by Levonyan & Trouni (1977, 1978). The corresponding solutions for both the Bragg and Laue geometries in perfect and deformed crystals based on the Laplace transformation of the time-dependent equations are presented by means of the Green function formalism by Levonyan & Trouni (1978). In particular, the explicit forms of solutions in perfect and uniformly bent crystals are presented. The solutions in perfect crystals for an incident infinite plane wavefront pulse are analysed for both the Laue and Bragg geometries by Levonyan & Trouni (1979). Concerning the new-generation X-ray synchrotron sources and XFELs, linear dynamical diffraction of X-ray pulses in crystals has also been investigated (He & Wark, 1993; Chukhovskii & Förster, 1995; Wark & Lee, 1999; Missalla *et al.*, 1999; Shastri *et al.*, 2001*a*,*b*; Graeff, 2002, 2004; Bushuev, 2008, 2009, 2011, 2013; Bushuev & Samoylova, 2011). The cases of incident δ-functions and Gaussians in time pulses are considered for both the Bragg and Laue geometries.

The nonlinear diffraction of monochromatic X-rays is also investigated. Nazarkin *et al.* (2003), using the cold collisionless plasma model, studied the linear dynamical diffraction of the formed X-ray second-order harmonic in a perfect crystal under the two-wave diffraction conditions. The backward

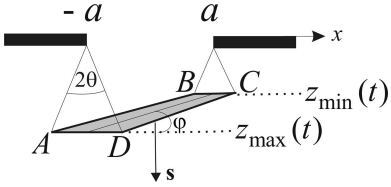

influence of the two Bragg-diffracted waves on the amplitude of the incident wave is not considered. Tamasaku & Ishikawa (2007*a*,*b*), without using the cold plasma model, investigated the kinematical diffraction of an X-ray plane wave under the second-order nonlinearity conditions with the parametric down conversion of an X-ray photon into an X-ray low-frequency photon and a UV photon. Conti *et al.* (2008), using the third-order nonlinear cold plasma model, investigated the direct propagation of an intense X-ray beam. Starting from the wave equation for a monochromatic component and replacing the linear susceptibility by the third-order nonlinear one, the nonlinear Takagi's equations in perfect and deformed crystals can be obtained as well (Balyan, 2015*a*,*b*). In those papers the third-order nonlinear dynamical diffraction of monochromatic X-ray waves was investigated.

Other X-ray nonlinear effects (two-photon absorption, radiation damage, and so on) have been investigated as well (Tamasaku *et al.*, 2014; Doumy *et al.*, 2011; Son *et al.*, 2011, and references therein).

XFELs will emit X-ray bunches of duration 100–200 fs (see, for example, Bushuev, 2008, and references therein). These bunches will have an irregular multi-peak structure. Each peak is a pulse (sub-pulse) with a Gaussian time amplitude. The preliminary phases and the amplitudes of the pulses (sub-pulses) randomly change from pulse to pulse. Each pulse is spatially full coherent. The sub-pulses have duration 0.1–0.2 fs separated by time intervals 0.3–0.5 fs. We shall consider the time-dependent diffraction of a pulse (sub-pulse). Until diffraction of a single pulse or a bunch is considered, thermal heating and radiation damage of the crystal may be ignored [for thermal heating during the diffraction see Bushuev (2013) and for radiation damage see Son *et al.* (2011)].

In this paper the third-order nonlinear time-dependent Takagi's equations are obtained. The crystal, as in the linear theory of diffraction, is considered as an isotropic medium. A method of solving these equations is presented for both the linear and nonlinear diffraction cases. Based on this method the solutions of the time-dependent equations are presented. The ultra-short pulse and the definite-duration Gaussian pulse cases are analyzed. The wavefront of the incident pulse, in contrast to other works, is restricted in the diffraction plane. Based on numerical calculations, the nonlinear time-dependent dynamical diffraction is compared with the linear diffraction case.

2. Derivation of the third-order nonlinear time-dependent Takagi's equations

In the general case the incident wave is a wave-packet, containing frequencies near a frequency $\omega_0 > 0$. In a nonlinear non-magnetic medium the wave equation for the electrical field strength $\tilde{\tilde{\mathbf{E}}}(\mathbf{r}, t)$ is (Boyd, 2003)

$$\mathrm{rot\,rot}\,\tilde{\tilde{\mathbf{E}}} + \frac{1}{c^2}\frac{\partial^2 \tilde{\tilde{\mathbf{E}}}}{\partial t^2} = -\frac{1}{\varepsilon_0 c^2}\frac{\partial^2 \tilde{\tilde{\mathbf{P}}}}{\partial t^2}, \tag{1}$$

where the polarization $\tilde{\tilde{\mathbf{P}}}(\mathbf{r}, t) = \tilde{\tilde{\mathbf{P}}}^{(1)}(\mathbf{r}, t) + \tilde{\tilde{\mathbf{P}}}^{(3)}(\mathbf{r}, t)$ is presented as the sum of the linear and the third-order nonlinear ones, c is the velocity of light in free space and ε_0 is the permittivity of free space. Let us present $\tilde{\tilde{\mathbf{E}}}(\mathbf{r}, t)$ and the polarizations as Fourier integrals,

$$\begin{aligned}\tilde{\tilde{\mathbf{E}}}(\mathbf{r}, t) &= \frac{1}{2\pi}\int_{-\infty}^{\infty} \tilde{\mathbf{E}}(\mathbf{r}, \omega)\exp(-i\omega t)\,\mathrm{d}\omega,\\ \tilde{\tilde{\mathbf{P}}}^{(1,3)}(\mathbf{r}, t) &= \frac{1}{2\pi}\int_{-\infty}^{\infty} \tilde{\mathbf{P}}^{(1,3)}(\mathbf{r}, \omega)\exp(-i\omega t)\,\mathrm{d}\omega.\end{aligned} \tag{2}$$

$\tilde{\tilde{\mathbf{E}}}(\mathbf{r}, t)$ and $\tilde{\tilde{\mathbf{P}}}(\mathbf{r}, t)$ are real quantities. From here and equation (2) it follows that $\tilde{\mathbf{E}}(\mathbf{r}, \omega) = \tilde{\mathbf{E}}^*(\mathbf{r}, -\omega)$ and $\tilde{\mathbf{P}}(\mathbf{r}, \omega) = \tilde{\mathbf{P}}^*(\mathbf{r}, -\omega)$. For the linear polarization, $\tilde{\mathbf{P}}^{(1)}(\mathbf{r}, \omega) = \varepsilon_0\chi^{(1)}(\mathbf{r}, \omega)\tilde{\mathbf{E}}(\mathbf{r}, \omega)$. The crystal may be considered as an isotropic medium. In isotropic media the linear susceptibility $\chi^{(1)}(\mathbf{r}, \omega)$ is a scalar. According to equations (1) and (2) the propagation equation for $\tilde{\mathbf{E}}(\mathbf{r}, \omega)$ will be

$$\mathrm{rot\,rot}\,\tilde{\mathbf{E}}(\mathbf{r}, \omega) - k(\omega)^2\left[1 + \chi^{(1)}(\mathbf{r}, \omega)\right]\tilde{\mathbf{E}}(\mathbf{r}, \omega) = \frac{k(\omega)^2}{\varepsilon_0}\tilde{\mathbf{P}}^{(3)}(\mathbf{r}, \omega) \tag{3}$$

where $k(\omega)^2 = \omega^2/c^2$. In the two-beam diffraction case,

$$\begin{aligned}\tilde{\tilde{\mathbf{E}}}(\mathbf{r}, t) = {}& \tilde{\mathbf{E}}_0(\mathbf{r}, t)\exp\left[i\mathbf{K}_0(\omega_0)\mathbf{r} - i\omega_0 t\right]\\ &+ \tilde{\mathbf{E}}_h(\mathbf{r}, t)\exp\left[i\mathbf{K}_h(\omega_0)\mathbf{r} - i\omega_0 t\right] + \text{c.c.}\end{aligned} \tag{4}$$

Here, c.c. means the complex conjugate quantity; $\tilde{\mathbf{E}}_0(\mathbf{r}, t)$ and $\tilde{\mathbf{E}}_h(\mathbf{r}, t)$ are the slowly varying amplitudes of the transmitted and the diffracted wave, respectively. The wavevectors are chosen so that they satisfy the exact Bragg condition $\mathbf{K}_0^2 = \mathbf{K}_h^2 = k(\omega_0)^2 = (2\pi/\lambda_0)^2$. Here λ_0 is the wavelength corresponding to the frequency ω_0. For the Fourier transforms we have

$$\mathbf{E}_{0,h}(\mathbf{r}, \omega) = \int_{-\infty}^{\infty} \tilde{\mathbf{E}}_{0,h}(\mathbf{r}, t)\exp(i\omega t)\,\mathrm{d}t. \tag{5}$$

For $\omega > 0$, taking the inverse-Fourier transform of equation (4), one finds

$$\begin{aligned}\tilde{\mathbf{E}}(\mathbf{r}, \omega) = {}& \mathbf{E}_0(\mathbf{r}, \omega - \omega_0)\exp(i\mathbf{K}_0\mathbf{r})\\ &+ \mathbf{E}_0^*(\mathbf{r}, -\omega - \omega_0)\exp(-i\mathbf{K}_0\mathbf{r})\\ &+ \mathbf{E}_h(\mathbf{r}, \omega - \omega_0)\exp(i\mathbf{K}_h\mathbf{r})\\ &+ \mathbf{E}_h^*(\mathbf{r}, -\omega - \omega_0)\exp(-i\mathbf{K}_h\mathbf{r})\\ \approx {}& \mathbf{E}_0(\mathbf{r}, \omega - \omega_0)\exp(i\mathbf{K}_0\mathbf{r})\\ &+ \mathbf{E}_h(\mathbf{r}, \omega - \omega_0)\exp(i\mathbf{K}_h\mathbf{r}).\end{aligned} \tag{6}$$

Here the approximation used is valid according to the assumption that the amplitudes are slowly varying functions on t and cannot have higher-order harmonics (Boyd, 2003). For $\omega < 0$, according to $\tilde{\mathbf{E}}(\mathbf{r}, \omega) = \tilde{\mathbf{E}}^*(\mathbf{r}, -\omega)$ and equation (6), $\tilde{\mathbf{E}}(\mathbf{r}, \omega) \approx \mathbf{E}_0^*(\mathbf{r}, -\omega - \omega_0)\exp(-i\mathbf{K}_0\mathbf{r}) + \mathbf{E}_h^*(\mathbf{r}, -\omega - \omega_0)\exp(-i\mathbf{K}_h\mathbf{r})$.

On the other hand,

$$\tilde{\tilde{\mathbf{P}}}^{(3)}(\mathbf{r},t)=\varepsilon_0\int\limits_{-\infty}^{\infty}\kappa^{(3)}(\tau_1,\tau_2,\tau_3)\,\tilde{\tilde{\mathbf{E}}}(\mathbf{r},t-\tau_1)\times\tilde{\tilde{\mathbf{E}}}(\mathbf{r},t-\tau_2)\,\tilde{\tilde{\mathbf{E}}}(\mathbf{r},t-\tau_3)\,\mathrm{d}\tau_1\,\mathrm{d}\tau_2\,\mathrm{d}\tau_3,\quad(7)$$

where $\kappa^{(3)}$ is the third-order nonlinear response function and is a fourth-rank tensor (Boyd, 2003). From (2) and (7),

$$\tilde{\mathbf{P}}^{(3)}(\mathbf{r},\omega)=\frac{1}{(2\pi)^2}\,\varepsilon_0\int\limits_{-\infty}^{\infty}\chi^{(3)}(\omega;\omega_1,\omega_2,\omega-\omega_1-\omega_2,\mathbf{r})\times\tilde{\mathbf{E}}(\mathbf{r},\omega_1)\mathbf{E}(\mathbf{r},\omega_2)\tilde{\mathbf{E}}(\mathbf{r},\omega-\omega_1-\omega_2)\,\mathrm{d}\omega_1\,\mathrm{d}\omega_2,\quad(8)$$

where the fourth-rank tensor of the susceptibility

$$\chi^{(3)}(\omega;\omega_1,\omega_2,\omega-\omega_1-\omega_2,\mathbf{r})=\int\limits_{-\infty}^{\infty}\kappa^{(3)}(\tau_1,\tau_2,\tau_3,\mathbf{r})\exp(i\omega_1\tau_1)\exp(i\omega_2\tau_2)\times\exp\big[i(\omega-\omega_1-\omega_2)\tau_3\big]\,\mathrm{d}\tau_1\,\mathrm{d}\tau_2\,\mathrm{d}\tau_3.\quad(9)$$

In (3), near the Bragg condition, the approximations $k(\omega)^2\approx[2(\omega-\omega_0)\omega_0+\omega_0^2]/c^2$ and $k(\omega)^2\chi^{(1)}(\mathbf{r},\omega)\approx k(\omega_0)^2\chi^{(1)}(\mathbf{r},\omega_0)$ are valid. Additionally, on the right-hand side of equation (3), $k(\omega)\approx k(\omega_0)$. After these approximations, equation (3) takes the form

$$\mathrm{rot\,rot}\,\tilde{\mathbf{E}}(\mathbf{r},\omega)-\frac{2(\omega-\omega_0)\omega_0}{c^2}\,\tilde{\mathbf{E}}(\mathbf{r},\omega)-k(\omega_0)^2\big[1+\chi^{(1)}(\mathbf{r},\omega_0)\big]\tilde{\mathbf{E}}(\mathbf{r},\omega)=\frac{k(\omega_0)^2}{\varepsilon_0}\tilde{\mathbf{P}}^{(3)}(\mathbf{r},\omega).\quad(10)$$

Multiplying (10) by $\exp[-i(\omega-\omega_0)t]/(2\pi)$ and integrating over $\omega-\omega_0$ in the limits $(-\infty,\infty)$, we obtain

$$\mathrm{rot\,rot}\,\mathbf{E}(\mathbf{r},t)-k(\omega_0)^2\big[1+\chi^{(1)}(\mathbf{r},\omega_0)\big]\,\mathbf{E}(\mathbf{r},t)-2ik(\omega_0)\frac{\partial\mathbf{E}(\mathbf{r},t)}{c\partial t}=\frac{k(\omega_0)^2}{\varepsilon_0}\int\limits_{-\infty}^{\infty}\tilde{\mathbf{P}}^{(3)}(\mathbf{r},\omega)\exp\big[-i(\omega-\omega_0)t\big]/(2\pi)\,\mathrm{d}(\omega-\omega_0).\quad(11)$$

Here,

$$\mathbf{E}(\mathbf{r},t)=\tilde{\mathbf{E}}_0(\mathbf{r},t)\exp(i\mathbf{K}_0\mathbf{r})+\tilde{\mathbf{E}}_h(\mathbf{r},t)\exp(i\mathbf{K}_h\mathbf{r}).\quad(12)$$

In the integral (8) the main contributions give the regions $\Delta_{1,2,3}$ near the three pairs of frequencies $(\omega_1=\omega_2=\omega_0)$, $(\omega_1=-\omega_0,\omega_2=\omega_0)$ and $(\omega_1=\omega_0,\omega_2=-\omega_0)$. Under the Bragg diffraction conditions the susceptibilities at these three pairs of frequencies may be taken out under the integral signs. Then one may use the intrinsic permutation symmetry (Boyd, 2003) $\chi^{(3)}_{ijkl}(\omega_0;\omega_0,\omega_0,-\omega_0,\mathbf{r})=\chi^{(3)}_{ijlk}(\omega_0;\omega_0,-\omega_0,\omega_0,\mathbf{r})=\chi^{(3)}_{ilkj}(\omega_0;-\omega_0,\omega_0,\omega_0,\mathbf{r})$. After these manipulations it may be shown that

$$\int\limits_{-\infty}^{\infty}\tilde{P}_i^{(3)}(\mathbf{r},\omega)\exp\big[-i(\omega-\omega_0)t\big]/(2\pi)\,\mathrm{d}(\omega-\omega_0)=3\varepsilon_0\chi^{(3)}_{ijkl}(\omega_0;\omega_0,\omega_0,-\omega_0,\mathbf{r})\,E_j(\mathbf{r},t)\,E_k(\mathbf{r},t)E_l^*(\mathbf{r},t),\quad(13)$$

where over all the dummy indices the summation is performed. The indices i, j, k and l can have values 1, 2 and 3, corresponding to the Cartesian coordinates x, y and z, respectively. From (11) and (13),

$$\mathrm{rot\,rot}\,\mathbf{E}(\mathbf{r},t)-k(\omega_0)^2\big[1+\chi^{(1)}(\mathbf{r},\omega_0)\big]\mathbf{E}(\mathbf{r},t)-2ik(\omega_0)\frac{\partial\mathbf{E}(\mathbf{r},t)}{c\partial t}=\frac{k(\omega_0)^2}{\varepsilon_0}\mathbf{P}^{(3)}(\mathbf{r},\omega_0,t),\quad(14)$$

where

$$\mathbf{P}^{(3)}(\mathbf{r},\omega_0,t)=\varepsilon_0A(\mathbf{r},\omega_0)\mathbf{E}(\mathbf{E}\mathbf{E}^*)+\varepsilon_0B(\mathbf{r},\omega_0)\mathbf{E}^*(\mathbf{E}\mathbf{E}).\quad(15)$$

In (15), $A=3\chi^{(3)}_{1122}+3\chi^{(3)}_{1221}$, $B=3\chi^{(3)}_{1221}$. According to the classical theory of polarization, $\chi^{(3)}_{1122}=\chi^{(3)}_{1221}$ and $A=6\chi^{(3)}_{1122}$ (Boyd, 2003). Using (14), repeating the deduction of the third-order nonlinear Takagi's equations (Balyan, 2015*a*) and introducing the amplitudes $E'_{0,h}=\tilde{E}_{0,h}\exp[-ik\chi_0^{(1)}z/(2\cos\theta)]$, the following third-order nonlinear time-dependent Takagi's equations (σ-polarization) are obtained,

$$\begin{aligned}&\frac{2i}{k}\frac{\partial E'_0}{\partial s_0}+\frac{2i}{k}\frac{\partial E'_0}{c\partial t}+\Big[\eta_0^{(3)}\Big(\big|E'_0\big|^2+\big|E'_h\big|^2\Big)+\eta_h^{(3)}E'_0E'^{*}_h+\eta_{\tilde{\boldsymbol{h}}}^{(3)}E'^{*}_0E'_h\Big](-\mu z/\cos\theta)E'_0\\&+\Big\{\chi_{\tilde{\boldsymbol{h}}}^{(1)}+\Big[\eta_0^{(3)}E'_0E'^{*}_h+\eta_{\tilde{\boldsymbol{h}}}^{(3)}\Big(\big|E'_0\big|^2+\big|E'_h\big|^2\Big)+\eta_{2\tilde{\boldsymbol{h}}}^{(3)}E'^{*}_0E'_h\Big]\\&\times\exp(-\mu z/\cos\theta)\Big\}E'_h=0,\end{aligned}\quad(16)$$

$$\begin{aligned}&\frac{2i}{k}\frac{\partial E'_h}{\partial s_h}+\frac{2i}{k}\frac{\partial E'_h}{c\partial t}+\Big[\eta_0^{(3)}\Big(\big|E'_0\big|^2+\big|E'_h\big|^2\Big)+\eta_h^{(3)}E'_0E'^{*}_h+\eta_{\tilde{\boldsymbol{h}}}^{(3)}E'^{*}_0E'_h\Big]\exp(-\mu z/\cos\theta)E'_h\\&+\Big\{\chi_h^{(1)}+\Big[\eta_0^{(3)}E'^{*}_0E'_h+\eta_h^{(3)}\Big(\big|E'_0\big|^2+\big|E'_h\big|^2\Big)+\eta_{2h}^{(3)}E'_0E'^{*}_h\Big]\\&\times\exp(-\mu z/\cos\theta)\Big\}E'_0=0,\end{aligned}$$

where $k\equiv k(\omega_0)$, $\eta^{(3)}=A(\mathbf{r},\omega_0)+B(\mathbf{r},\omega_0)$, $\chi^{(1)}\equiv\chi^{(1)}(\mathbf{r},\omega_0)$, $\mu=k\chi_{0i}^{(1)}$ is the linear absorption coefficient of the crystal, s_0 and s_h are the coordinates along the propagation directions of the transmitted and diffracted waves, respectively, θ is the Bragg angle, $\chi_{0,h}^{(1)}$ are the Fourier coefficients of the linear susceptibility for the diffraction vectors 0 and $\mathbf{h}$, respectively, $\eta_{0,h,2h}^{(3)}$ are the corresponding Fourier coefficients of the third-order nonlinear part of the susceptibility, the z axis is oriented along the reflecting planes, and the x axis is oriented anti-parallel to the diffraction vector $\mathbf{h}$.

2.1. Third-order nonlinear time-dependent Takagi's equations form in the stationary frame

Boyd (2003) described a method of solving the nonlinear diffraction equations in visible-light optics for the one-beam diffraction case. In this method the problem is solved by passing to the stationary frame of diffraction. Here we modify this method to be suited for the Bragg time-dependent diffraction case. In the Bragg diffraction case we have two coupled equations and the method cannot be directly applied. Let us introduce the retarded time $\tau=t-z/(c\cos\theta)=t-(s_0+s_h)/c$. Let us note that, in visible-light optics, in the expression of the retarded time, instead of z the coordinate along the propagation direction of the beam is taken; in adition, c is taken instead of $c\cos\theta$ (Boyd, 2003). Now the

amplitudes are functions of (x, z, τ) or (s_0, s_h, τ), *i.e.* $E'_{0,h}(x, z, t) \equiv E'_{0,h}(s_0, s_h, t) = E_{0,hs}(x, z, \tau) \equiv E_{0,hs}(s_0, s_h, \tau)$. The differentiations in (16), $\partial E'_{0,h}/\partial s_{0,h} = \partial E_{0,hs}/\partial s_{0,h} + (\partial E_{0,hs}/\partial\tau)(\partial\tau/\partial s_{0,h}) = \partial E_{0,hs}/\partial s_{0,h} - \partial E_{0,hs}/c\partial\tau$ and $\partial E'_{0,h}/\partial t = \partial E_{0,hs}/\partial\tau$, bring the time-dependent equations (16) to the stationary third-order nonlinear Takagi's equations,

$$\begin{aligned}
&\frac{2i}{k}\frac{\partial E_{0s}}{\partial s_0} + \left[\eta_0^{(3)}\left(\left|E_{0s}\right|^2 + \left|E_{hs}\right|^2\right) + \eta_h^{(3)}E_{0s}E_{hs}^*\right.\\
&\left. + \eta_{\tilde{h}}^{(3)}E_{0s}^*E_{hs}\right]\exp(-\mu z/\cos\theta)E_{0s}\\
&+ \left\{\chi_{\tilde{h}}^{(1)} + \left[\eta_0^{(3)}E_{0s}E_{hs}^* + \eta_{\tilde{h}}^{(3)}\left(\left|E_{0s}\right|^2 + \left|E_{hs}\right|^2\right) + \eta_{2\tilde{h}}^{(3)}E_{0s}^*E_{hs}\right]\right.\\
&\left.\times\exp(-\mu z/\cos\theta)\right\}E_{hs} = 0, \qquad (17)\\
&\frac{2i}{k}\frac{\partial E_{hs}}{\partial s_h} + \left[\eta_0^{(3)}\left(\left|E_{0s}\right|^2 + \left|E_{hs}\right|^2\right) + \eta_h^{(3)}E_{0s}E_{hs}^*\right.\\
&\left. + \eta_{\tilde{h}}^{(3)}E_{0s}^*E_{hs}\right]\exp(-\mu z/\cos\theta)E_{hs}\\
&+ \left\{\chi_h^{(1)} + \left[\eta_0^{(3)}E_{0s}^*E_{hs} + \eta_h^{(3)}\left(\left|E_{0s}\right|^2 + \left|E_{hs}\right|^2\right) + \eta_{2h}^{(3)}E_{0s}E_{hs}^*\right]\right.\\
&\left.\times\exp(-\mu z/\cos\theta)\right\}E_{0s} = 0.
\end{aligned}$$

Equations (17) may be integrated numerically using the half-step algorithm (Authier, 2001; Epelboin, 1977); but in equation (17) the effective Fourier-coefficients of the susceptibility are functions of the amplitudes. This difficulty can be overcome if, for each step of the calculations, at the exit surface of a layer the obtained amplitudes at the entrance surface of the same layer are used for evaluating the effective Fourier-coefficients of the susceptibility. This method is called the modified half-step algorithm (Balyan, 2015*a*,*b*). It will be noted that solving of the third-order nonlinear time-dependent Takagi's equations (16) by means of the Fourier method will bring to the integral equation (11), which is very difficult to solve numerically or analytically. In the case of deformed crystals, including time-dependent deformations, in (17), one must replace $\chi_{\mathbf{g}}$ by $\chi_{\mathbf{g}}\exp(-i\mathbf{gu})$ and $\eta_{\mathbf{g}}$ by $\eta_{\mathbf{g}}\exp(-i\mathbf{gu})$. Here $\mathbf{g}$ is an arbitrary vector of the reciprocal lattice and $\mathbf{u}$ is the displacement vector of atoms from their equilibrium positions in the ideal crystal. Thus, these cases may also be solved analytically and numerically using the stationary equations (17).

3. Linear time-dependent diffraction of an X-ray pulse restricted in the diffraction plane wavefront

Usually the time-dependent equations (16) in the linear case ($\eta^{(3)} = 0$) are solved by performing the Fourier or Laplace transformations of the amplitudes (Levonyan & Trouni, 1978; Chukhovskii & Förster, 1995). After finding the solution of the obtained equations by means of the Green function, the Fourier or Laplace transforms of the solutions give the solutions of (16). Here the equations (16) for the linear case are solved by passing to the linear case stationary equations (17). The Fourier or Laplace transformations are not used. The linear form of (17) has the form of the standard stationary Takagi's equations. Let us for simplicity consider the symmetrical Laue-case of diffraction, σ-polarization. According to the Green function formalism (Takagi, 1969; Authier, 2001; Pinsker, 1982),

$$E_{hs}(x, z, \tau) = \int_{-\infty}^{+\infty} G(x - x', z)\, E_{0s}(x', 0, \tau)\, \mathrm{d}x', \qquad (18)$$

where the Green function

$$\begin{aligned}
G(x, z) = {} & ik\chi_h^{(1)}J_0\left[\pi\cot\theta\left(z^2\tan^2\theta - x^2\right)^{1/2}/\Lambda\right]\\
& \times H(z\tan\theta - |x|)/4\sin\theta. \qquad (19)
\end{aligned}$$

Here $\Lambda = \lambda\cos\theta/[\chi_h^{(1)}\chi_{\tilde{h}}^{(1)}]^{1/2}$ and $\Lambda_r = \mathrm{Re}\,\Lambda = \lambda\cos\theta/|\chi_{hr}^{(1)}|$ is the extinction length in linear theory. It is necessary to determine $E_{0s}(x', 0, \tau)$. Since τ is fixed, then $\tau = t - z/(c\cos\theta) = t_0$. Here t_0 at $z = 0$ corresponds to t at depth z. According to the definition, $E'_0(x, 0, t_0) = E_{0s}(x, 0, \tau)$. The incident wave has the form

$$E_0^{(i)}(x, t) = E_0(x)F_0(t - x\sin\theta/c)\exp\left[iK_{0x}^{(i)}x\right] \qquad (20)$$

(see, for example, Bushuev, 2008), where $K_{0x}^{(i)} = k\sin(\theta + \Delta\theta)$ and $\Delta\theta$ is the deviation from the Bragg exact angle. At the moment $t = 0$ the centre of the incident pulse intercepts the origin of the coordinate system. The origin is situated on the entrance surface of the crystal. Using the continuity conditions on the entrance surface and equation (20) one finds

$$\begin{aligned}
E'_0(x, 0, t_0) &= E_0(x)F_0\left[t_0 - x/(c\sin\theta)\right]\exp(ik\cos\theta\Delta\theta x)\\
&= E_{0s}(x, 0, \tau). \qquad (21)
\end{aligned}$$

Inserting (21) into (18) brings

$$\begin{aligned}
E_{hs}(x, z, \tau) = {} & \int_{-\infty}^{+\infty} G(x - x', z)\exp(ik\cos\theta\Delta\theta x')\\
& \times E_0(x')F_0(\tau - x'\sin\theta/c)\,\mathrm{d}x', \qquad (22)
\end{aligned}$$

and finally

$$\begin{aligned}
\tilde{E}_h(x, z, t) = {} & \exp\left[ik\chi_0^{(1)}z/(2\cos\theta)\right]\\
& \times \int_{-\infty}^{+\infty} G(x - x', z)\exp(ik\cos\theta\Delta\theta x')\\
& \times E_0(x')F_0[t - z/(c\cos\theta) - x'\sin\theta/c]\,\mathrm{d}x'. \qquad (23)
\end{aligned}$$

3.1. Diffraction of an incident Gaussian time pulse

Consider the incident wave to be Gaussian in time (Bushuev, 2008) and the wavefront of the incident beam to be planar. The size of the incident beam in the diffraction plane along the entrance surface of the crystal is in the range $(-a, a)$, *i.e.*

$$\begin{aligned}
E_0(x) &= E_{0i}[H(x + a) - H(x - a)],\\
F_0(t) &= \exp\left(-t^2/\tau_0^2\right). \qquad (24)
\end{aligned}$$

Here E_{0i} is the constant amplitude of the incident pulse and $H(x)$ is the Heaviside step-function. Let us denote the intensity of the incident pulse as $I_i = |E_{0i}|^2$. In contrast with other

works we consider the time-dependent diffraction for incident waves with a definite size wavefront in the diffraction plane. Inserting (24) into (23),

$$\tilde{E}_h(x, z, t) = \exp\left[ik\chi_0^{(1)} z/(2\cos\theta)\right] \times \int_{\max[-a, x-z\tan\theta]}^{\min[a, x+z\tan\theta]} G(x-x', z)\exp(ik\cos\theta\Delta\theta x') \times \exp\left[-(x'-x_\tau)^2\sin^2\theta/c^2\tau_0^2\right]\mathrm{d}x', \quad (25a)$$

where

$$x_\tau = c\tau/\sin\theta. \quad (25b)$$

3.1.1. Diffraction of an ultra-short pulse. An important case of the incident wave is the ultra-short pulse case (Chukhovskii & Förster, 1995). The formula (25*a*) brings to the solution (the function G may be taken out under the integral sign at the point $x' = x_\tau$)

$$\tilde{E}_h(x, z, t) = \left(\sqrt{\pi}c\tau_0/\sin\theta\right)\exp\left[ik\chi_0^{(1)} z/(2\cos\theta)\right] \times G(x-x_\tau, z)\exp(ik\cos\theta\Delta\theta x_\tau)\, E_0(x_\tau). \quad (26)$$

From the expression $E_0(x_\tau)$ of (24) and from (26) we conclude that the field is non-zero when $-a < x_\tau < a$. Thus at a fixed depth z the field exists in the time interval

$$-a\sin\theta/c + z/(c\cos\theta) < t < a\sin\theta/c + z/(c\cos\theta). \quad (27)$$

Correspondingly for a fixed t the field exists in the following interval of z,

$$z_{\min}(t) < z < z_{\max}(t), \quad (28)$$

where $z_{\min}(t) = \max[0, -a\sin 2\theta/2 + ct\cos\theta]$, $z_{\max}(t) = a\sin 2\theta/2 + ct\cos\theta$. From (28) it follows that for a fixed t the pulse length Δ_z along the z axis is

$$\Delta_z(|t| \le a\sin\theta/c) = a\sin 2\theta/2 + ct\cos\theta, \quad \Delta_z(t \ge a\sin\theta/c) = a\sin 2\theta. \quad (29)$$

For a fixed t the boundaries $z_{\min,\max}(t)$ of the pulse are determined by (28). For $t > a\sin\theta/c$ these boundaries move at velocity $\mathrm{d}z/\mathrm{d}t = c\cos\theta$. Thus, the velocity of the pulse along the z axis is $c\cos\theta$. As follows from (27), the back-front of the pulse emerges from the crystal at the moment $t_{\max} = (T/\cos\theta + a\sin\theta)/c$. Here T is the thickness of the crystal.

Inside the boundaries (28), the pulse form and the intensity, according to (26), are determined by the behaviour of the Green function. As follows from (19) and (26), the field is non-zero when $|x - x_\tau| < z\tan\theta$. Combining this condition and the condition (27), one finds

$$\sin\theta\max[-a, x - z\tan\theta]/c + z/(c\cos\theta) < t < \sin\theta\min[a, x + z\tan\theta]/c + z/(c\cos\theta). \quad (30)$$

Thus, the pulse duration at a fixed point (x, z) is different in the different regions of the diffraction (Fig. 1). According to (25*a*) these regions are obtained by means of the characteristics passed through the edges of the slit as in the stationary theory (Slobodetskii & Chukhovskii, 1970). For the whole

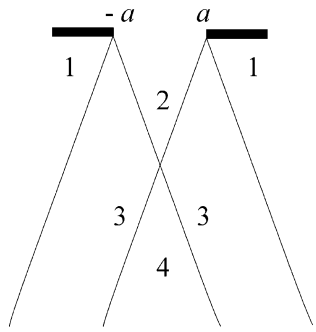

Figure 1
Diffraction regions of a definite-size incident plane wavefront pulse inside the crystal.

time of the diffraction at depth z the field is non-zero in the limits $-a - z\tan\theta < x < a + z\tan\theta$ (Fig. 1). In region 1 of Fig. 1 the amplitude of the pulse electrical field is zero for all times of observation [formula (25*a*)]. According to (30) the pulse duration in region 2 at a fixed point is $2z\tan\theta\sin\theta/c$, in region 3 it is $(z\tan\theta + a)\sin\theta/c$ and finally in region 4 it is $2a\sin\theta/c$. From $|x - x_\tau| < z\tan\theta$ it follows that for a given z and a given t the field is non-zero in the base of the triangle with the aperture angle 2θ. The apex of the triangle is at the point $-a \le x_\tau \le a$ on the entrance surface and the width of the triangle base along the x axis is $2z\tan\theta$. Inserting the expression (25*b*) of x_τ into the condition $|x - x_\tau| < z\tan\theta$, one finds

$$ct/\sin\theta - 2z(1 + \sin^2\theta)/\sin 2\theta < x < ct/\sin\theta - z\cot\theta. \quad (31)$$

Let us determine the form of the pulse for $t \ge a\sin\theta/c$ (by the same way the moments $|t| \le a\sin\theta/c$ may be analyzed as well). According to (31) on the back-front $z = z_{\min}(t)$ of the pulse we have

$$-ct\sin\theta + a\left(1 + \sin^2\theta\right) < x < ct\sin\theta + a\cos^2\theta. \quad (32a)$$

Thus, the coordinate of the centre of the pulse on the back-front is

$$x_c(z_{\min}) = a. \quad (32b)$$

On the face-front $z = z_{\max}(t)$ of the pulse

$$-ct\sin\theta - a(1 + \sin^2\theta) < x < ct\sin\theta - a\cos^2\theta, \quad (33a)$$

and consequently

$$x_c(z_{\max}) = -a. \quad (33b)$$

Thus the x coordinates of the centres of the pulse on the back- and on the face-fronts do not depend on time. The line connecting the centres is inclined with respect to the x axis by an angle φ given by the relation

$$\tan\varphi = \left[z_{\max}(t) - z_{\min}(t)\right]/\left[x_c(z_{\min}) - x_c(z_{\max})\right] = (1/2)\sin 2\theta. \quad (34)$$

In Fig. 2 the diffracted pulse form $ABCD$ for a fixed time $t > a\sin\theta/c$ is presented. This form of the diffracted pulse is obtained using (29) and (31)–(34). In Fig. 2, $AD = 2z_{\max}\tan\theta$ is

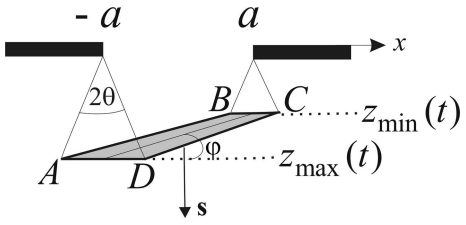

Figure 2
Diffracted pulse form $ABCD$ inside the crystal for a fixed time $t > a\sin\theta/c$. Incident ultra-short pulse case. AD and BC are parallel to the x axis. The inclination angle φ of the pulse is shown. The arrow **s** is directed along the z axis and indicates the propagation direction of the pulse.

parallel to $BC = 2z_{\min}\tan\theta$. Since $AD > BC$ then AB is not parallel to CD. Thus the pulse has a trapezoidal form.

In the same way it may be established that for $|t| \leq a\sin\theta/c$ the form of the pulse is a triangle. In this case BC (Fig. 2) is reduced to a point which is situated on the entrance surface of the crystal. This point lies between the points $(-a, 0)$ and $(a, 0)$ and its x coordinate is $x = ct/\sin\theta$. The base of the triangle is AD. The inclination angle is determined by the same relation (34) as for the previous case. For $t < -a\sin\theta/c$ the field inside the crystal is zero.

For details of the inclination angle and the form of the pulse for the case of an incident infinite wavefront pulse, see Bushuev (2008) and Graeff (2002), respectively.

3.1.2. Diffraction of a pulse with definite duration. As follows from (25*a*) the diffraction region inside the crystal may be divided into four regions [as for monochromatic waves (Slobodetskii & Chukhovskii, 1970)]. These regions are shown in Fig. 1 and have been mentioned in the previous section. The diffracted pulse form, the duration and the inclination angle will be approximately the same as for an ultra-short pulse if $c\tau_0/\sin\theta \ll a$. For the case $a \to 0$ (simultaneously $c\tau_0/\sin\theta \gg a$), according to (25*a*),

$$\tilde{E}_h(x, z, t) \approx 2a\exp\left[ik\chi_0^{(1)}z/(2\cos\theta)\right] \times G(x, z)\exp\left[-x_\tau^2\sin^2\theta/\left(c^2\tau_0^2\right)\right]. \quad (35)$$

According to (35) the inclination angle is zero. The pulse propagates along the z axis with velocity $c\cos\theta$. The pulse for a fixed z fills the triangle's base having aperture angle 2θ. The apex of the triangle is situated at the point $(0, 0)$. The pulse duration is $2\tau_0$ and its longitudinal size along z is $2\tau_0 c\cos\theta$. This is the pulse duration at a fixed point (x, z) as well. Thus, the inclination angle and the pulse duration inside the crystal are functions on the aperture of the used slit.

3.2. Propagation of the pulse in free space

The pulse propagation in free space has been discussed by Bushuev (2008) and Kohn (2012). The discussion in those papers is based on the Fourier transform of the pulse electrical field strength. Below an approach is given based on the pulse propagation equation in the frame in which the pulse is nearly stationary (Boyd, 2003). Inserting (4) into (1) and taking the polarization equal to zero, the following propagation equation in free space is obtained for the diffracted wave slowly varying amplitude,

$$\Delta\tilde{E}_h(x, y, z, t) + 2ik\frac{\partial\tilde{E}_h(x, y, z, t)}{\partial s_h} + 2ik\frac{\partial\tilde{E}_h(x, y, z, t)}{c\partial t} - \frac{\partial^2\tilde{E}_h(x, y, z, t)}{c^2\partial t^2} = 0. \quad (36)$$

Using the retarded time $\tau_1 = t - \varsigma/c$, where $\varsigma = -x\sin\theta + (z - T)\cos\theta$ and passing to the amplitude $\tilde{E}_h(x, y, z, t) = E_{hs}(x, y, z, \tau_1)$ from (35) one finds the propagation equation in the frame in which the pulse is nearly stationary,

$$\partial^2E_{hs}/\partial y^2 + \partial^2E_{hs}/\partial x^2 + \partial^2E_{hs}/\partial z^2 + 2ik\frac{\partial\left[1 + (i/\omega_0)\partial/\partial\tau\right]E_{hs}}{\partial s_h} = 0. \quad (37)$$

Near the exit surface of the crystal, equation (37) is approximately

$$\frac{\partial E_{hs}}{\partial s_h} = 0. \quad (38)$$

According to (38) and the continuity conditions on the exit surface of the crystal,

$$E_h(x, y, z, t) = \tilde{E}_h^{(e)}[x + (z - T)\tan\theta, y, T, t - (z - T)/(c\cos\theta)]. \quad (39)$$

Here the superscript (e) indicates the field on the exit surface of the crystal [formulas (25*a*) and (26)].

The Fourier spectrum $F_h(\omega)$ of the amplitude (39) is essential. It may be compared with the Fourier spectrum of the incident wave. For an ultra-short pulse using expression (26) one finds

$$F_h(\omega) = \left(ik\chi_h^{(1)}\sqrt{\pi}\tau_0/4\sin\theta\right)\exp\left[ik\chi_0^{(1)}T/(2\cos\theta)\right] \times \exp\left\{i\omega[T/(c\cos\theta) + \varsigma/c]\right\} \times \int_{\max(-a, -T\tan\theta)}^{\min(a, T\tan\theta)} J_0\left[\pi\cot\theta(T^2\tan^2\theta - t^2)^{1/2}/\Lambda\right] \times \exp(i\omega t\sin\theta/c)\,dt. \quad (40)$$

When $a \geq T\tan\theta$ one may use the corresponding tabular integral (Prudnikov *et al.*, 1986). In this case

$$F_h(\omega) = i\sqrt{\pi}\tau_0\sqrt{\chi_h^{(1)}/\chi_{\bar{h}}^{(1)}}\exp\left[ik\chi_0^{(1)}T/(2\cos\theta)\right] \times \sin\left\{\left(\pi T/\Lambda\right)\sqrt{\left[2\omega\sin^2\theta/\left(\sqrt{\chi_{\bar{h}}^{(1)}\chi_h^{(1)}}\omega_0\right)\right]^2 + 1}\right\} \Big/ \sqrt{\left[2\omega\sin^2\theta/\left(\sqrt{\chi_{\bar{h}}^{(1)}\chi_h^{(1)}}\omega_0\right)\right]^2 + 1}. \quad (41)$$

The frequency range $|\Delta\omega/\omega_0| = [\chi_{\bar{h}}^{(1)}\chi_h^{(1)}]^{1/2}/\sin^2\theta$ effectively exists in the spectrum of the diffracted wave. In the case $a < T\tan\theta$ the integration may be performed only numerically; but when $a < \Lambda\tan\theta/\pi$ the Bessel function may be

taken out under the integral sign at the point $t = 0$ and in this case

$$F_h(\omega) \approx \left[2ika\sqrt{\pi}\tau_0\chi_h^{(1)}/4\sin\theta\right] \times \exp\left[ik\chi_0^{(1)}T/(2\cos\theta)\right]\exp\left\{i\omega[T/(c\cos\theta)+\varsigma/c]\right\} \times J_0(\pi T/\Lambda)\sin(\omega a\sin\theta/c)/(\omega a\sin\theta/c). \quad (42)$$

The frequency range is determined from the relation

$$\left|\Delta\omega/\omega_0\right| = 2\pi c/(\omega_0 a\sin\theta). \quad (43)$$

The analyses of the pulse form and of the pulse duration may be performed as that inside the crystal. As already mentioned, the back-front of the pulse emerges from the crystal at the moment $t_{\max} = (T/\cos\theta + a\sin\theta)/c$. The analyses show that for $t > t_{\max}$ the centers of the back- and of the face-fronts $x_c + (z - T)\tan\theta = \pm a$ move with velocity $-c\sin\theta$ along the x axis and move with velocity $c\cos\theta$ along the z axis. The pulse form outside the crystal is the same as that inside the crystal (Fig. 2), but outside the crystal $AD = BC = 2T\tan\theta$ and AB is parallel to CD. The height of the pulse along the z axis is the same as that inside the crystal and is equal to $a\sin 2\theta$ [see formula (29)]. The inclination angle of the pulse is given by the same relation (34) as inside the crystal. So, outside the crystal the pulse form is a parallelogram. This parallelogram near the exit surface of the crystal without changing its dimensions moves along the propagation direction of the diffracted wave with velocity c.

4. Third-order nonlinear time-dependent diffraction of an X-ray pulse restricted in the diffraction plane wavefront

After analyzing the linear case let us pass to the third-order nonlinear time-dependent diffraction case. The third-order nonlinear time-dependent Takagi's equations (16) may be solved by passing to the stationary third-order nonlinear Takagi's equations (17) and using the modified half-step algorithm. The boundary conditions (20) must be used. We will compare the results of the linear and third-order nonlinear time-dependent equations in all regions of the diffraction (Fig. 1) for incident Gaussian time pulses. The time will be presented in fs units, the x coordinate in units of $\Lambda_r\tan\theta$ and z coordinate in units of Λ_r. The intensities will be given in units of $I_{\rm cr}/3$, where $I_{\rm cr}$ is the critical intensity. For this value of the intensity the contribution of the nonlinear part of the scattering equals that of the linear one [(Balyan, 2015*a*,*b*); in these references the value of $I_{\rm cr}$ is also estimated]. We shall consider the dependence of the diffracted pulse reflectivity on time at a fixed observation point (x_0, z_0),

$$R_h^t(x_0, z_0, t) = \left|\tilde{E}_h(x_0, z_0, t)\right|^2/I_i. \quad (44)$$

Let us introduce the time-integrated transmission coefficient,

$$T_0(x_0, z_0) = \frac{\int_{-\infty}^{\infty}\left|\tilde{E}_0(x_0, z_0, t)\right|^2 {\rm d}t}{I_i\int_{-\infty}^{\infty}\exp(-2t^2/\tau_0^2)\,{\rm d}t} = \left(\frac{2}{\pi}\right)^{1/2}\frac{\int_{-\infty}^{\infty}\left|\tilde{E}_0(x_0, z_0, t)\right|^2 {\rm d}t}{I_i\tau_0} \quad (45)$$

and the time-integrated reflection coefficient

$$R_h(x_0, z_0) = \left(\frac{2}{\pi}\right)^{1/2}\frac{\int_{-\infty}^{\infty}\left|\tilde{E}_h(x_0, z_0, t)\right|^2 {\rm d}t}{I_i\tau_0} = \left(\frac{2}{\pi}\right)^{1/2}\frac{\int_{-\infty}^{\infty}R_h^t(x_0, z_0, t)\,{\rm d}t}{\tau_0}. \quad (46)$$

The results will be obtained using the numerical integration of (17) both for the linear and nonlinear cases. The incident pulse duration $\tau_0 = 0.2$ fs (short pulse). Two cases of the slit widths will be considered: $a = 10$ and $a = 1$. The reflection Si(220) for the wavelength $\lambda = 0.71$ Å (17.46 keV) is taken. The intensity of the incident pulse $I_i = 0.5$ (in units of $I_{\rm cr}/3$). Let us, for the case $a = 10$ ($\sim$70 µm), take three observation points $(-a, 1.5)$, $(0, 1.5)$ and $(a, 1.5)$. The first and the third points of the observation are in region 3 and the second point is in region 2 (Fig. 1). The depth is $z_0 = 1.5\Lambda_r \approx 55$ µm.

The numerical calculated reflectivity dependence (44) on time is shown in Fig. 3. Fig. 3(*a*) depicts the reflectivity at the point $(-a, 1.5)$, Fig. 3(*b*) at the observation point $(0, 1.5)$ and Fig. 3(*c*) at the observation point $(a, 1.5)$. In all figures the dashed lines correspond to the linear case and the solid lines to the nonlinear case. As can be seen in Fig. 3(*a*), the intensity dependence and the duration are the same for both the linear and nonlinear cases, but the reflectivity in the nonlinear case is less than that in the linear case. For point $(0, 1.5)$ (Fig. 3*b*) the duration for linear and nonlinear cases is the same, but the form of the pulse is different. In contrast to the case of Fig. 3(*a*), the pulse form at the point $(a, 1.5)$ is different for linear and nonlinear cases.

In Fig. 4 the reflectivity (44) is shown for the case $a = 1$ ($\sim$7 µm) at the observation point $(0, 1.5)$. This observation point lies in region 4 (Fig. 1). As can be seen in this figure, the pulse form is different for the linear and nonlinear cases but the duration is the same.

In Figs. 5(*a*), 5(*b*) and 5(*c*) for the case $a = 10$ the dependence of the time-integrated intensities (45) and (46) on the intensity of the incident wave at the points $(-a, 1.5)$, $(0, 1.5)$ and $(a, 1.5)$, respectively, are shown. These time-integrated intensities correspond to the regions of Figs. 4(*a*), 5(*b*) and 5(*c*), respectively. As can be seen from these figures, the energy flux is concentrated in the transmission direction (Fig. 5*c*).

In Fig. 6 the time-integrated intensities are shown for $a = 1$ at the point $(0, 1.5)$. These time-integrated intensities correspond to the diffraction region of Fig. 4.

The behavior of the time-integrated transmission coefficient is not monotonic; meanwhile the time-integrated reflection coefficient monotonously decreases.

Summarizing, one may say that for the short incident pulse case the pulse duration in all regions of the observation is the

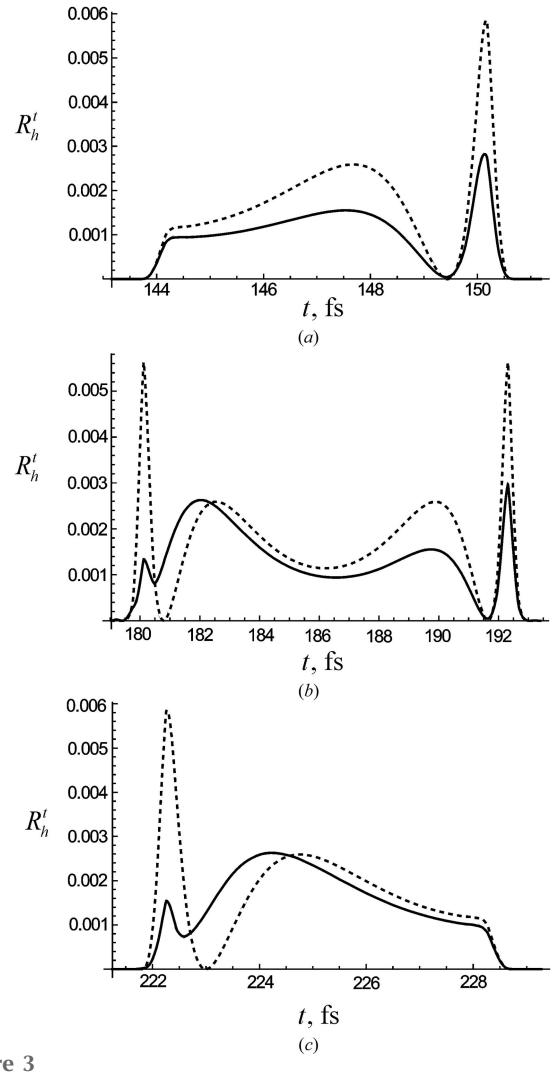

Figure 3
Temporal dependence of the diffracted pulse reflectivity R_h^t at a fixed observation point inside the crystal. Si(220) reflection; $\lambda = 0.71$ Å; $\tau_0 = 0.2$ fs; $a = 10$. The coordinates of the fixed observation points are (*a*) $(-a, 1.5)$, (*b*) $(0, 1.5)$ and (*c*) $(a, 1.5)$. Dashed curve: linear diffraction; solid curve: nonlinear diffraction. Intensity of the incident pulse $I_i = 0.5$. Numerical calculation.

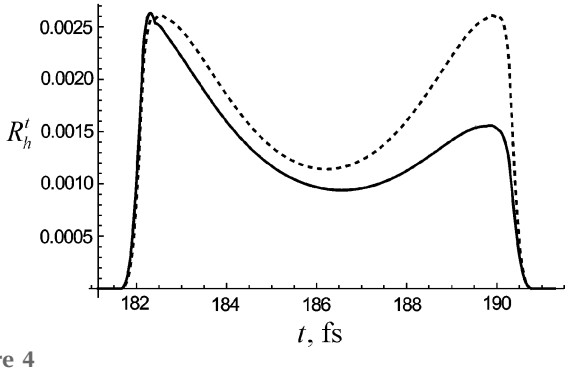

Figure 4
Temporal dependence of the diffracted pulse reflectivity R_h^t inside the crystal at a fixed point. Si(220) reflection; $\lambda = 0.71$ Å; $\tau_0 = 0.2$ fs; $a = 1$; coordinate of the fixed point $(0, 1.5)$. Dashed curve: linear diffraction; solid curve: nonlinear diffraction. Intensity of incident pulse $I_i = 0.5$. Numerical calculation.

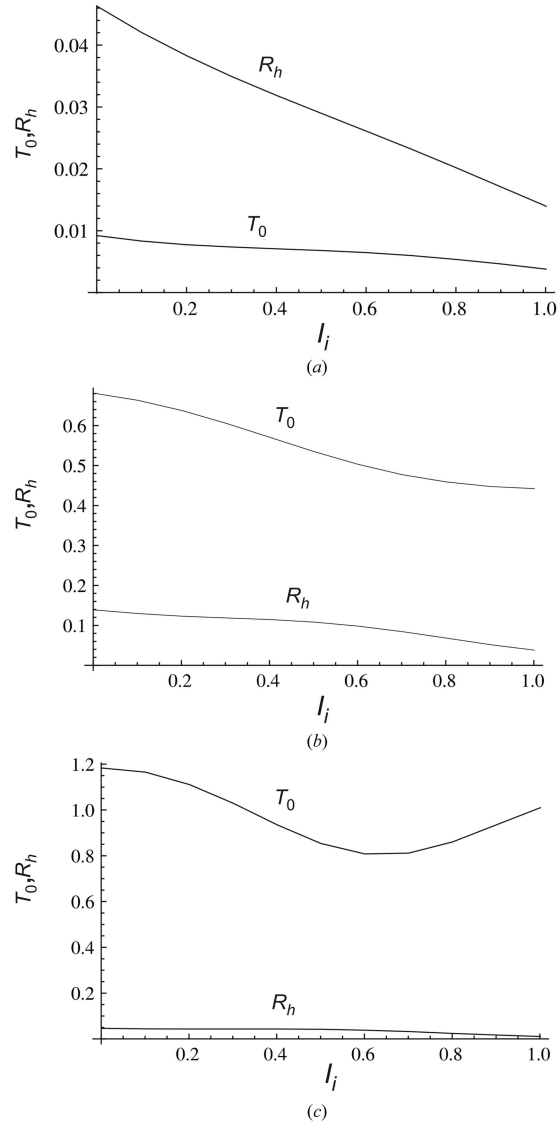

Figure 5
Time-integrated transmission and reflection coefficients dependences on the intensity of the incident wave at a fixed point inside the crystal. Si(220) reflection; $\lambda = 0.71$ Å; $\tau_0 = 0.2$ fs; $a = 10$. Coordinates of the fixed observation points are (*a*) $(-a, 1.5)$, (*b*) $(0, 1.5)$ and (*c*) $(a, 1.5)$.

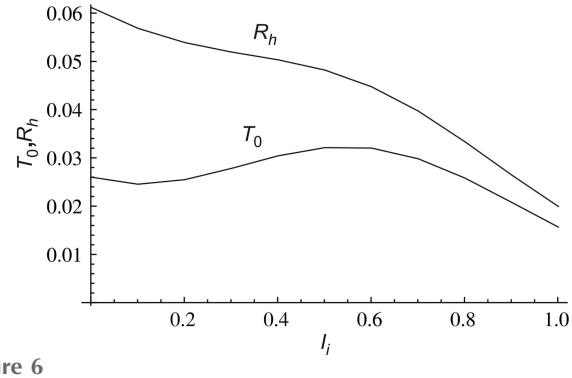

Figure 6
Time-integrated transmission and reflection coefficients dependences on the intensity of the incident wave at a fixed point inside the crystal. Si(220) reflection; $\lambda = 0.71$ Å; $\tau_0 = 0.2$ fs; $a = 1$. Coordinates of the fixed observation point are $(0, 1.5)$.

same for both the linear and nonlinear cases. In the left-hand region 3 (Fig. 1) the pulse form is the same for both the linear and nonlinear cases, but the reflectivity for the nonlinear case is less. In all other regions the pulse forms for linear and nonlinear cases are different. In Figs. 3(*b*), 3(*c*) and 4, self-steepening of the pulse form in the nonlinear case takes place (Boyd, 2003).

The main explanation of these features of the nonlinear diffraction is based on the self-induced deviation from the Bragg condition in the nonlinear case. This parameter is one of the main parameters for the Bragg diffraction features. Comparing the third-order nonlinear stationary equations (17) with the linear theory equations written in the form with the deviation parameter from the Bragg condition (Authier, 2001; formulas 11.5a, 11.5b and 11.6), one may say that the self-induced deviation angle $\Delta\theta_{\rm eff}$ is proportional to $[\eta_0^{(3)}(|E_{0s}|^2 + |E_{hs}|^2) + \eta_h^{(3)}E_{0s}E_{hs}^* + \eta_{\bar{h}}^{(3)}E_{0s}^*E_{hs}]\exp(-\mu z/\cos\theta)$ in equations (17*a*) and (17*b*). In (17*a*), $\chi_{\bar{h}}^{(1)}$ is replaced by the self-induced Fourier-coefficient of the susceptibility,

$$\chi_{\bar{h}}^{(1)} \rightarrow \chi_{\bar{h}}^{(1)} + \left[\eta_0^{(3)}E_{0s}E_{hs}^* + \eta_{\bar{h}}^{(3)}\left(\left|E_{0s}\right|^2 + \left|E_{hs}\right|^2\right) + \eta_{2\bar{h}}^{(3)}E_{0s}^*E_{hs}\right] \times \exp(-\mu z/\cos\theta),$$

and, in (17*b*), $\chi_h^{(1)}$ is replaced by the self-induced Fourier-coefficient of the susceptibility,

$$\chi_h^{(1)} \rightarrow \chi_h^{(1)} + \left[\eta_0^{(3)}E_{0s}E_{hs}^* + \eta_h^{(3)}\left(\left|E_{0s}\right|^2 + \left|E_{hs}\right|^2\right) + \eta_{2h}^{(3)}E_{0s}^*E_{hs}\right] \times \exp(-\mu z/\cos\theta).$$

The self-induced parameter from the Bragg condition brings about an asymmetry of the rays with the positive and negative signs of this parameter, whereas the self-induced Fourier-coefficients bring about the reduction of the scattering power, since $\chi_h^{(1)}$ and $\eta^{(3)}$ have opposite signs (Balyan, 2015*a*,*b*).

The values of the Fourier coefficients of the susceptibility of the linear theory are taken from Pinsker (1982). For the Fourier coefficients of the real part of the nonlinear susceptibility the relations $\eta_{0r}^{(3)} = 3|\chi_{0r}^{(1)}|/I_{\rm cr}$, $\eta_{hr}^{(3)} = 3|\chi_{hr}^{(1)}|/I_{\rm cr}$ are used (Balyan, 2015*a*,*b*). For the Fourier coefficients of the imaginary parts of the nonlinear susceptibility, $\eta_{0,hi}^{(3)}/\eta_{0,hr}^{(3)} = 0.01$ values are taken. These values are almost equal to the same ratio of the linear part.

5. Summary

Based on the model of the scattering of X-rays on bound electrons, the third-order nonlinear time-dependent Takagi's equations are obtained. These equations, in the particular case of linear polarization, are the time-dependent linear Takagi's equations. A new analytical and numerical method of solving the time-dependent Takagi's equations both for the linear and nonlinear cases is presented. Based on this method, the case of an incident Gaussian time pulse with a restricted plane wavefront in the diffraction plane is considered. For linear diffraction the cases of an infinitely short pulse and of a definite duration pulse are analyzed. The forms of the pulse inside the crystal and in free space are presented. It is shown that the inclination angle of the pulse with respect to the direction of the diffraction vector is a function on the width of the slit used. Using the modified half-step algorithm the results of numerical calculations of the reflectivity dependence on time at a fixed observation point are presented. The diffraction region is divided into four regions. In each region the dependence of the intensity on time has its own behavior that is different for the linear and nonlinear cases. In the nonlinear case the self-induced deviation parameter from the Bragg exact angle brings about an asymmetry of the time-dependent intensity and to self-steepening.

The experiments may be performed using X-ray synchrotron sources and XFELs.

References

Authier, A. (2001). *Dynamical Theory of X-ray Diffraction.* Oxford: University Press.

Balyan, M. K. (2015*a*). *Crystallogr. Rep.* **60**, 993–1000.

Balyan, M. K. (2015*b*). *J. Synchrotron Rad.* **22**, 1410–1418.

Boyd, R. (2003). *Nonlinear Optics.* New York: Academic.

Bushuev, V. A. (2008). *J. Synchrotron Rad.* **15**, 495–505.

Bushuev, V. A. (2009). *Bull. Russ. Acad. Sci. Phys.* **73**, 52–56.

Bushuev, V. A. (2013). *Bull. Russ. Acad. Sci. Phys.* **77**, 15–20.

Bushuev, V. A. & Samoylova, L. (2011). *Crystallogr. Rep.* **56**, 819–827.

Bushuev, V., Samoylova, L., Sinn, H. & Tschentscher, Th. (2011). *Proc. SPIE*, **8141**, 81410T.

Chukhovskii, F. N. & Förster, E. (1995). *Acta Cryst.* A**51**, 668–672.

Conti, C., Fratalocchi, A., Ruocco, G. & Sette, F. (2008). *Opt. Express*, **16**, 8324–8331.

Doumy, G., Roedig, C., Son, S.-K., Blaga, C. I., DiChiara, A. D., Santra, R., Berrah, N., Bostedt, C., Bozek, J. D., Bucksbaum, P. H., Cryan, J. P., Fang, L., Ghimire, S., Glownia, J. M., Hoener, M., Kanter, E. P., Krässig, B., Kuebel, M., Messerschmidt, M., Paulus, G. G., Reis, D. A., Rohringer, N., Young, L., Agostini, P. & DiMauro, L. F. (2011). *Phys. Rev. Lett.* **106**, 083002.

Epelboin, Y. (1977). *Acta Cryst.* A**33**, 758–767.

Graeff, W. (2002). *J. Synchrotron Rad.* **9**, 82–85.

Graeff, W. (2004). *J. Synchrotron Rad.* **11**, 261–265.

He, H. & Wark, J. S. (1993). Report RAL-93–031. Rutherford Appleton Laboratory, Oxford, England.

Kohn, V. G. (2012). *J. Synchrotron Rad.* **19**, 84–92.

Levonyan, L. V. & Trouni, K. G. (1977). *Proceedings of IV Conference on Dynamical Effects of X-rays and Electrons Scattering*, 31 March–2 April 1976, Leningrad, Russia, pp. 17–22. (In Russian.)

Levonyan, L. V. & Trouni, K. G. (1978). *Proc. Natl. Acad. Sci. Armen. Phys.* **13**, 108–113. (In Russian.)

Levonyan, L. V. & Trouni, K. G. (1979). *Proc. Natl. Acad. Sci. Armen. Phys.* **14**, 253–260. (In Russian.)

Missalla, T., Uschmann, I., Förster, E., Jenke, G. & von der Linde, D. (1999). *Rev. Sci. Instrum.* **70**, 1288–1299.

Nazarkin, A., Podorov, S., Uschmann, I., Förster, E. & Sauerbrey, R. (2003). *Phys. Rev. A*, **67**, 041804.

Pinsker, Z. G. (1982). *X-ray Crystal Optics.* Moscow: Nauka (In Russian.)

Prudnikov, A. P., Brychkov, Y. A. & Marichev, O. I. (1986). *Integrals and Series*, Vol. 2. New York: Gordon and Breach.

Shastri, S. D., Zambianchi, P. & Mills, D. M. (2001*a*). *J. Synchrotron Rad.* **8**, 1131–1135.

Shastri, S. D., Zambianchi, B. & Mills, D. M. (2001*b*). *Proc. SPIE*, **4143**, 69–77.

Slobodetskii, I. Sh. & Chukhovskii, F. N. (1970). *Crystallography*, **15**, 1101–1107. (In Russian.)

Son, S.-K., Chapman, H. N. & Santra, R. (2011). *Phys. Rev. Lett.* **107**, 218102.
Takagi, S. (1969). *J. Phys. Soc. Jpn*, **26**, 1239–1253.
Tamasaku, K. & Ishikawa, T. (2007*a*). *Phys. Rev. Lett.* **98**, 244801.
Tamasaku, K. & Ishikawa, T. (2007*b*). *Acta Cryst.* A**63**, 437–438.
Tamasaku, K., Shigemasa, E., Inubushi, Y., Katayama, T., Sawada, K., Yumoto, H., Ohashi, H., Mimura, H., Yabashi, M., Yamauchi, K. & Ishikawa, T. (2014). *Nat. Photon.* **8**, 313–316.
Wark, J. S. & Lee, R. W. (1999). *J. Appl. Cryst.* **32**, 692–703.